arXiv:1603.08998v2 [physics.chem-ph] 8 Apr 2016

Rates and singlet/triplet ratios from TADF transients

Mitchell C. Nelson*

(Dated: 15 March 2016)

Thermally activated delayed fluorescence has been reported in a number of OLED emitter materials engineered to have low singlet-triplet energy gaps. Here we derive closed solutions for steady state and transient behaviors, and apply these results to obtain the singlet and triplet relaxation, forward and reverse crossing rates and the gap energy and reverse crossing prefactor from delayed and prompt relaxation rates measured over a series of temperatures. The primary rates are then used to calculate the fluorescent/phosphorescent ratio and the singlet/triplet population ratio. The method avoids the need for gated yield measurements. Good fits are obtained using previously published data for 4CzIPN and m-MTDATA:t-Bu-PBD and the results appear to be consistent with reported quantities were available, and with reported behaviors of OLEDS that use these materials.

I. INTRODUCTION

Thermally activated fluorescence (TADF) is seen as a strategy for improving OLED efficiency by harvesting excitation energy from slowly relaxing phosphorescent states via reverse intersystem crossing (RISC) to faster relaxing, more efficient singlet states. [1, 3–8] Materials engineered to implement TADF have been reported to achieve as high as 100% internal quantum efficiency with large reverse crossing rates and low singlet-triplet energy gaps.[4, 5, 7] Yet, singlet/triplet ratios and relaxation rates are determined by at least four parameters comprising the individual relaxation rates and intersystem crossing rates. Direct observation of these rates has been considered difficult.[8]

Singlet-triplet energy gaps have been obtained from the temperature dependence of reverse crossing rates where the reverse rates are calculated from prompt and delayed yields and decay rates and a supplied value for the forward crossing rate.[2, 3] In this work we describe a method for finding the singlet and triplet relaxation rate constants, the forward and reverse intersystem crossing rate constants, and the singlet-triplet energy gap and prefactor governing the reverse intersystem crossing rate constant, using only the temperature dependent decay rates. The ratio of fluorescence to phosphorescence, and the ratio of singlets to triplets, in steady state electroluminescence and

*Correspondence: drmcnelsonm@gmail.com

phototransients, can then be calculated from the four primary rate constants.

In Section II, we model the system in a pair of linear differential equations which we solve to obtain the steady state behavior, and the time dependent behavior following from a short photoexcitation into the singlet. Then in Section III, we apply our model to re-analyze published TADF data for two materials to recover their primary relaxation and crossing rates and the reversing crossing parameters. The results are found to be in agreement with reported values where available and consistent with observed behaviors.

II. TADF

We consider behaviors in two regimes, continuously driven systems as in electroluminescence, and transient luminescence as follows from photoexcitation by a subnanosecond laser pulse. Closed form solutions are found for both regimes in terms of four primary rates: relaxation from the singlet and from the triplet, and forward and reverse intersystem crossing. Temperature dependence, scaled by the singlet-triplet gap energy, enters through the thermally activated reverse crossing rate and provides a route to extract the primary parameters from empirical decay rates.

Electroluminescence occurs when charge carriers (electrons and holes) are combined onto a site where they form an excited state that can decay and emit light.[9] Charge carriers arrive with random spin and so a mixed population of singlet and triplet excited states is formed, as illustrated in FIG. 1.

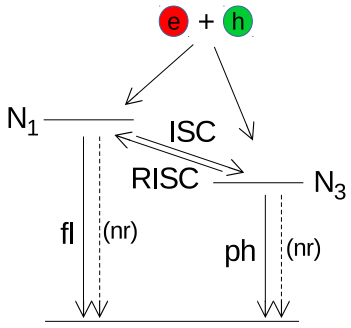

FIG. 1: Electroluminescence where charge carrier recombination forms a mix of singlets (N_1) and triplets (N_3), with fluorescent (fl) and nonradiative (nr) relaxation from the singlets, phosphorescent (ph) and nonradiative relaxation from the triplets, and intersystem crossing between singlets and triplets in the forward (ISC) and reverse (RISC) directions.

Rate equations for our empirical case can be written as[12]

$$\dot{n} = \frac{\gamma}{eV} I - k_{eh} n^2 N_0 \tag{1}$$

$$\dot{N_1} = \eta_{S/T} k_{eh} n^2 N_0 - (k_1 + k_{isc}) N_1 + k_{risc} N_3 \tag{2}$$

$$\dot{N_3} = (1 - \eta_{S/T}) k_{eh} n^2 N_0 - (k_3 + k_{risc}) N_3 + k_{isc} N_1 \tag{3}$$

where γI is the recombination current, e is the charge on an electron, V is the effective volume, k_{eh} is the recombination rate constant, n is the free charge carrier density, N_0 is the ground state population (per unit volume), N_1 is the singlet excited state population, N_3 is the triplet excited state population, $\eta_{S/T}$ is the fraction of singlets produced by recombination, k_1 is the singlet relaxation rate with $k_1 = k_{fl} + k_{1,nr}$ where k_{fl} is rate of radiative relaxation from the singlet (fluorescence) and $k_{1,nr}$ is the rate of nonradiative 1st order relaxation from the singlet, and similarly, k_3 is the relaxation rate from the triplet with $k_3 = k_{ph} + k_{3,nr}$ where k_{ph} is rate of radiative relaxation from the triplet (phosphorescence) and $k_{3,nr}$ is the rate of nonradiative 1st order relaxation from the triplet, k_{isc} is the forward intersystem crossing rate and k_{risc} is reverse intersystem crossing rate. For the present analysis we consider a simple system at low power where higher order losses can be omitted.[1]

In steady state, the ratio of the singlet and triplet populations is obtained as

$$\frac{N_1}{N_3} = \frac{\eta_{S/T} + k_{risc}/k_3}{(1 - \eta_{S/T}) + k_{isc}/k_1} \frac{k_3}{k_1} \tag{4}$$

and the ratio of fluorescent to phosphorescent output is

$$\frac{L_1}{L_3} = \frac{\eta_{S/T} + k_{risc}/k_3}{(1 - \eta_{S/T}) + k_{isc}/k_1} \frac{\phi_1 \ \chi_1}{\phi_3 \ \chi_3} \tag{5}$$

where $L_1 = k_{fl} N_1$ is the fluorescent output, $L_3 = k_{ph} N_3$ is the phosphorescent output, $\phi_1 = k_{fl}/k_1$ and $\phi_3 = k_{ph}/k_3$ are the radiative quantum yields for fluorescence and phosphorescence and χ_1 and χ_3 are the fraction of each that escape the device. In FIG. 2 the output ratio L_1/L_3 is shown as a function of k_{isc}/k_1 and k_{risc}/k_3. Fluorescence is stronger than phosphorescence in the quadrant where $k_{risc}/k_3 > 1$ and $k_{isc}/k_1 < 1$.

Temperature dependence enters the fluorescent and singlet ratios through k_{risc} which is usually thermally activated and follows an Arrhenius law,[10]

$$k_{risc} = \Phi \, \mathrm{e}^{-\Delta E_{S-T}/k_B T} \tag{6}$$

[1] Self- and charge-quenching losses in three level systems with crossings are discussed in detail in [13].

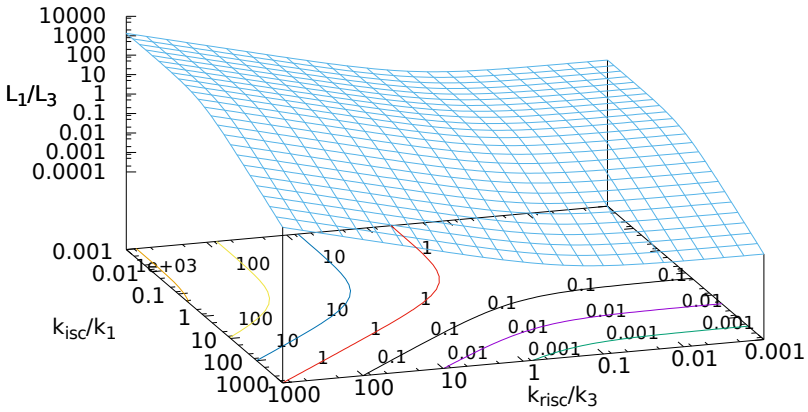

FIG. 2: Fluorescent/phosphorescent output ratio in steady state, as a function of forward and reverse crossing rates in dimensionless units scaled by the spontaneous relaxation rates per equation (5).

where dE is the singlet-triplet energy gap, k_B is Boltzmann's constant, T is the Kelvin temperature and the prefactor Φ is related to spin-orbit coupling mechanisms.[11] A change in temperature is then equivalent to moving along the surface in FIG. 2, in the direction indicated by the axis labeled k_{risc}/k_3.

Transient photoluminescence following sub-nanosecond laser excitation has been used to study several TADF materials.[3, 4] As we will show here, two new rate constants emerge in the transient relaxation from a pulsed input in these systems. The temperature dependence of the emergent rate constants provides an opportunity to obtain the four primary rate constants along with singlet-triplet energy gap and prefactor discussed above. We begin by finding the closed solution to the relaxation problem. For our purposes we are interested in the decay following from an initial state $N_1(0), N_3(0)$, as depicted in FIG. 3.

We write rate equations for the system as

$$\dot{N}_1 = -(k_1 + k_{isc})N_1 + k_{risc}N_3 \tag{7}$$

$$\dot{N}_3 = -(k_3 + k_{risc})N_3 + k_{isc}N_1 \tag{8}$$

which we will solve subject to initial conditions corresponding to the moment just following a fast pulse from a laser. We present the solution in some detail to illuminate an important behavior of the system.

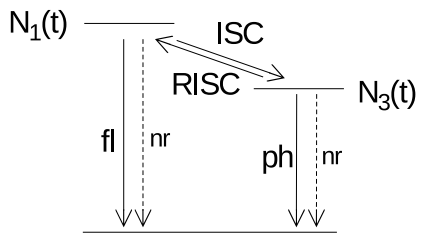

FIG. 3: Relaxation and intersystem crossing following photoexcitation, with fluorescent (fl) and nonradiative (nr) relaxation from the singlet and phosphorescent (ph) and nonradiative relaxation from the triplet, and forward (ISC) and reverse (RISC) intersystem crossings.

The rate equations can be written as $\dot{\vec{\mathrm{N}}} = \mathbf{A}\tilde{\mathrm{N}}$, where

$$\mathbf{A} = \begin{bmatrix} -(k_1 + k_{isc}) & k_{risc} \\ k_{isc} & -(k_3 + k_{risc}) \end{bmatrix} \tag{9}$$

We assume $\vec{N} = \vec{a}\mathrm{e}^{rt}$ are solutions of the system and find r and $\vec{a}$ as eigenvalues and eigenvectors of $|\mathbf{A} - \mathbf{I}\, r| = 0$. We thus have two decay constants, given by

$$r = \frac{1}{2}\left[Tr(\mathbf{A}) \pm \left(\mathrm{Tr}(\mathbf{A})^2 - 4\ \mathrm{Det}\mathbf{A}\right)^{1/2}\right] \tag{10}$$

Approximating the square root, we obtain the emergent rate constants,

$$r_1 \approx -\left(k_1 + k_{isc} + \frac{k_{isc}k_{risc}}{k_1 - k_3 + k_{isc} - k_{risc}}\right) \tag{11}$$

$$r_2 \approx -\left(k_3 + k_{risc} - \frac{k_{isc}k_{risc}}{k_1 - k_3 + k_{isc} - k_{risc}}\right) \tag{12}$$

The last term can be small so the fast rate constant r_1 is less sensitive to changes in k_{risc} compared to the slow rate constant r_2 which increases directly with an increase in k_{risc}. Eigenvectors can be found as

$$\mathbf{a_n} = \begin{pmatrix} k_{risc} \\ k_1 + k_{isc} + r_n \end{pmatrix} \tag{13}$$

or alternatively,

$$\mathbf{a_n} = \begin{pmatrix} k_3 + k_{risc} + r_n \\ k_{isc} \end{pmatrix} \tag{14}$$

General solutions, using either set of eigenvectors, are

$$\begin{pmatrix} N_1 \\ N_3 \end{pmatrix} = C_1\mathbf{a_1}\mathrm{e}^{r_1 t} + C_2\mathbf{a_2}\mathrm{e}^{r_2 t} \tag{15}$$

where C_1 and C_2 are chosen to satisfy initial conditions. The two emergent rate constants are thus shared by the singlet and the triplet.

Following excitation with a fast laser pulse at or above the singlet absorption, we expect an initial configuration $N_1(0) = 1, N_3(0) = 0$. Choosing the first option for our eigenvectors and applying the initial condition on the triplet we obtain

$$\frac{C_1}{C_2} = 1 + \frac{k_\Delta^2}{k_{isc}k_{risc}} \tag{16}$$

where $k_\Delta = (k_1 - k_3 + k_{isc} - k_{risc})$. Substituting this into (15), we obtain

$$\frac{N_1}{C_2} = \left(k_{risc} + \frac{k_\Delta^2}{k_{isc}}\right) \mathrm{e}^{r_1 t} + k_{risc}\, \mathrm{e}^{r_2 t} \tag{17}$$

$$\frac{N_3}{C_2} = \left[k_\Delta + \frac{k_{isc}k_{risc}}{k_\Delta}\right] \left(\mathrm{e}^{r_2 t} - \mathrm{e}^{r_1 t}\right) \tag{18}$$

During the time $t < 1/r_1$, the triplet population ramps up while the singlet decays, both at r_1, and then at some time $t >> 1/r_1$ both the singlet and triplet decay slowly at the shared rate r_2. The delayed luminescence therefore has a constant ratio of fluorescence and phosphorescence,

$$\frac{L_3}{L_1} \approx \left(\frac{k_{isc}}{k_\Delta} + \frac{k_\Delta}{k_{risc}}\right) \frac{k_3}{k_1} \tag{19}$$

(apart from a factor of $\phi_1\chi_1/\phi_3\chi_3$).

With a minor simplification, the prompt luminescence ($L_1 + L_3$) at sufficiently small t (compared to $1/r_1$) can be written as,

$$L_p = \left[\left(\frac{k_\Delta}{k_{isc}}k_1 - k_3\right) k_\Delta + \left(k_1 - \frac{k_{isc}}{k_\Delta}\right) k_{risc}\right] C_2\, \mathrm{e}^{-r_1 t} \tag{20}$$

and at sufficiently large t, the delayed luminescence can be written as,

$$L_d = \left[k_3 k_\Delta + \left(k_1 + k_3\frac{k_{isc}}{k_\Delta}\right) k_{risc}\right] C_2\, \mathrm{e}^{-r_2 t} \tag{21}$$

Thus the rate constants r_1 and r_2 are readily available by simply supplying a short laser pulse to excite the system into the singlet, and then measuring the decay lifetimes within a suitably prompt time interval and after some suitably delayed time interval.

It might be noted on examining equation (11) and equation (12), that

$$r_1 + r_2 = -(k_1 + k_3 + k_{isc} + k_{risc}) \tag{22}$$

Measuring r_1 and r_2 at several temperatures and then fitting the quantity $r_1 + r_2$, to $f(T) = a + \Phi \exp[-dE/kT]$, immediately yields the gap energy ΔE_{S-T} and the prefactor Φ for k_{risc}

in equation (6). In a similar manner, all of the primary constants (k_1, k_3, k_{isc} and k_{risc}, or ϕ and ΔE_{S-T}), can be obtained from simple curve fitting and combinations involving only the temperature dependent rate constants, as will be shown in the Section III.

An alternative method for obtaining k_{risc} and ΔE_{S-T} is based on delayed and prompt measurements of luminescent yields.[2, 3] Expanding the temperature dependence in equation (21), the general form for a delayed or prompt luminous yield is

$$Y(t_{gate}) \sim \left[a + b\,\mathrm{e}^{-(\Delta E_{S-T}/k_bT)}\right] \mathrm{e}^{-\left(\alpha+\beta\,\mathrm{e}^{-(\Delta E_{S-T}/k_bT)}\right)t_{gate}} \tag{23}$$

where the measurement is made in a small window centered on a time t_{gate}, and provided that t_{gate} is well within either the prompt or delayed range as described above. Note the second exponential in which appears both t_{gate}, and the exponential temperature dependence. In other words, the expected relationship between yield and temperature seen in the first term is modified by the combined temperature and time dependence seen in the second exponential term. This presents additional complications for measurement and for data reduction and fitting, compared to the rate-constant-only method described above.

In FIG. 4 the system of differential equations (7),(8) is integrated numerically to show the fluorescence to phosphorescence ratio L_1/L_3 evaluated at $t = 3/k_3$ as a function of k_{isc}/k_1 and k_{risc}/k_3 with $k_1 = 1, k_3 = 0.001$. The result closely aligns with direct evaluation of equation (19). Comparing this result to FIG. 2 we see that the delayed transient fluorescence/phosphorescence ratio is different in shape and has a larger range compared to the steady state ratio.

It is important to note that FIG. 2 and FIG. 4 display output ratios L_1/L_3. The excited state population ratio N_1/N_3 is lower by a factor of k_1/k_3, which can be order 10^3. From FIG. 2, the range for N_1/N_3 is from 1 to 10^{-6}.

This completes our model and closed form solutions for steady state and transient luminescence in a three level TADF system.

III. ANALYSIS OF TADF DATA

Delayed fluorescence transients, as we have shown, are characterized by a fast (prompt) rate constant r_1 and a slow (delayed) rate constant r_2. Here we describe a method for obtaining k_3, k_1, k_{isc}, k_{risc} and ΔE_{S-T} from r_1 and r_2 measured at several temperatures, and a second method by which ΔE_{S-T} and the prefactor Φ are obtained from $r_1 + r_2$. We then apply the methods to data published for two TADF materials and calculate the fluorescence/phosphorescence and

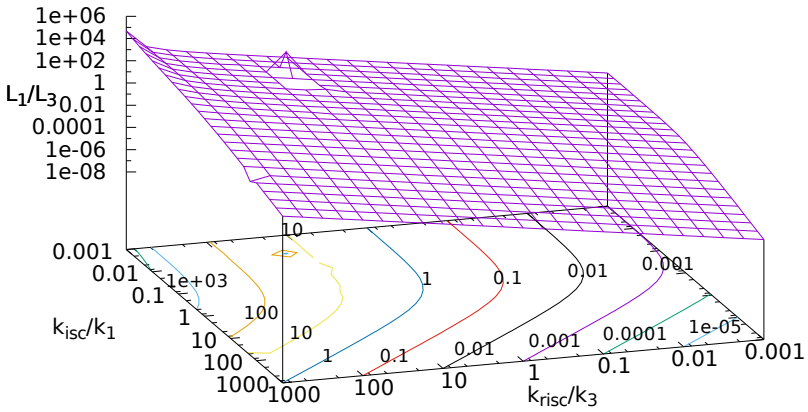

FIG. 4: Output ratio (single L_1 to triplet L_3) in delayed luminescence as a function of forward and reverse crossing rates in dimensionless units by scaling to spontaneous relaxation rates, $k_1 = 1, k_3 = 10^{-3}$.

singlet/triplet ratios using equation (5) and equation (19).

We can write equation (12) for r_2, as

$$-r_2 \approx k_3 + \left(1 - \frac{k_{isc}}{k_\Delta}\right) k_{risc} \approx k_3 + \phi_3 \, \mathrm{e}^{-\Delta E_{S-T}/k_B T} \tag{24}$$

provided that k_Δ is nearly constant, or equivalently that $k_1 + k_{isc} - k_3 >> k_{risc}$ which will generally be true since $k_1 >> k_3$. Fitting delayed decay rate data measured at several temperatures (c.f. FIG. 5(a) and 5(b)), then gives us k_3 and ΔE_{S-T} along with the quantity ϕ_3.

Similarly, we can write equation (11) for r_1, as

$$-r_1 \approx k_1 + k_{isc} + \frac{k_{isc}}{k_\Delta} k_{risc} = k_1 + k_{isc} + \phi_1 \, \mathrm{e}^{-\Delta E_{S-T}/k_B T} \tag{25}$$

Fitting prompt decay rate data measured at several temperatures (c.f. FIG. 5(c) and 5(d)), gives us the quantity $k_1 + k_{isc}$ and again ΔE_{S-T}, along with the quantity ϕ_1.

Summing equations (11) and (12) we have

$$r_1 + r_2 = -(k_1 + k_{isc} + k_3 + k_{risc}) \tag{26}$$

and we can now obtain k_{risc} by either of two methods. The first is that we simply add r_1 and r_2 measured at some temperature T, and subtract the already obtained quantities $k_1 + k_{isc}$ and k_3. Alternatively, we can write equation (26) as

$$-(r_1 + r_2) = (k_1 + k_{isc} + k_3) + \Phi \, \mathrm{e}^{-\Delta E_{S-T}/k_b T} \tag{27}$$

and then fit the temperature dependent quantity $r_1 + r_2$ to obtain k_{risc} explicitly in terms of its prefactor and gap energy (c.f. FIG. 6).

Then finally, we obtain k_{isc}, and k_1, from ϕ_1 and ϕ_3,

$$k_{isc} = k_\Delta \frac{\phi_1/\phi_3}{1 + \phi_1/\phi_3} \tag{28}$$

Fluorescent and singlet ratios can then be calculated from equations (5) and (19).

Prompt and delayed rate constants as a function of temperature are provided in Uoyama, et. al. (2012),[4] and Goushi, et. al. (2012),[3], in supplemental materials. Applying the above procedure to analyze the reported data, we obtain the values listed in Table I.

Material	$k_1(10^6)$	$k_{isc}(10^6)$	$k_3(10^3)$	$k_{risc}^{(RT)}(10^6)$	$\Phi(10^6)$	ΔE	L_1/L_3	N_1/N_3
4CzIPN	8.5	46	29	6.7	200	0.081	37 (36)	0.13 (0.12)
m-MTDATA:t-Bu-PBD	1.2	1.1	13	1.0	11	0.062	47 (43)	0.53 (0.48)

TABLE I: Values in seconds and electron-volts obtained using data provided in Uoyama 2012 and Goushi 2012 (Adachi, et. al.). Fluorescence and singlet ratios in the delayed transient are shown in parenthesis.

Examining the configuration of constants for the two materials, we see a large prefactor for the engineered material 4CzIPN along with a modestly larger gap energy compared to that in m-MTDATA:t-Bu-PBD, and find that the reverse crossing rates and population ratios are within an order of magnitude. The modest singlet/triplet ratios produce large flourescence/phosphorescence ratios because of the large k_1/k_3 ratios. High efficiency reported in OLEDS using these materials likely originates in competition between reverse crossing and losses in the triplet. Thus, charge and self-quenching losses in a conventional OLED architecture, will eventually outpace reverse crossing and produce roll-off.

The r_1 and r_2 fits are shown in FIG. 5. It might be noted that scatter is low in panels (a) and (b) where the rates are order $10^5/s$ and less, increases in panel (d) where the rates are order $10^6/s$ and increases again in panel (c) where the rates are $10^7/s$. Since the magnitude of the scatter (as well as on a percentage basis) is greater at the faster decay rate, the scatter might be related to gate timing as described above. The effect of the data scatter on the calculated singlet/triplet population is about 10%.

Uoyama et. al., for 4CzIPN report ΔE_{S-T} as 83 meV compared to our 81 meV, k_{risc} as 1.3×10^6/s at 300K, compared to our 6.7×10^6/s, and for k_{isc} they use 4×10^7 compared to our 4.6×10^7. Goushi, et. al., for m-MTDATA:t-Bu-PBD, report ΔE_{S-T} as 50 meV compared to our

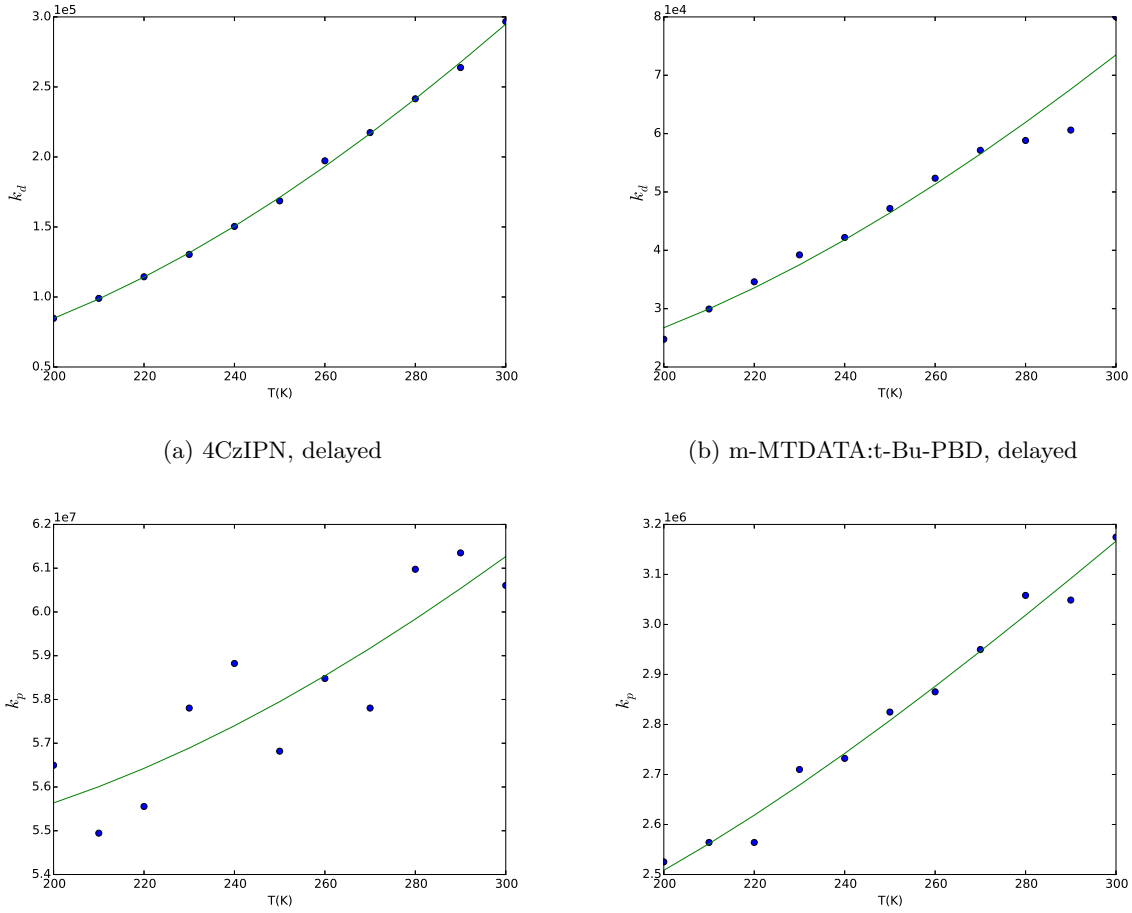

(a) 4CzIPN, delayed

(b) m-MTDATA:t-Bu-PBD, delayed

(c) 4CzIPN, prompt

(d) m-MTDATA:t-Bu-PBD, prompt

FIG. 5: Fit for delayed and prompt relaxation constants. Data are from supplemental materials provided by Goushi, et. al.[3] and Uoyama, et. al.[4].

60 meV, k_{risc} as 1.3×10^5 compared to our 1.0×10^6, and for k_{isc} they use 1.3×10^5 compared to our 1.0×10^6. Thus the values obtain in our analysis are similar to the previously reported values.

The earlier values were obtained by first calculating reverse crossing rates at each of a set of temperatures using the equation[3],

$$k_{risc} = \frac{k_p k_d \phi_d}{k_{isc}\phi_p} \tag{29}$$

where k_d and k_p are the delayed and prompt decay rates, ϕ_d and ϕ_p are the delayed and prompt yields, and k_{isc} is the supplied forward crossing rate. ΔE_{S-T} is then found as the slope in a log-linear fit to $1/k_B T$. For 4CzIPN, k_{risc} values are obtained with little scatter and ΔE_{S-T} is within a few percent of our value. For m-MTDATA:t-Bu-PBD, there is considerable scatter in the k_{risc} values and ΔE_{S-T} agrees less closely with our value. As noted above in discussing FIG. 5, there is more scatter in the prompt rate data for 4CzIPN compared to that of m-MTDATA:t-Bu-PBD,

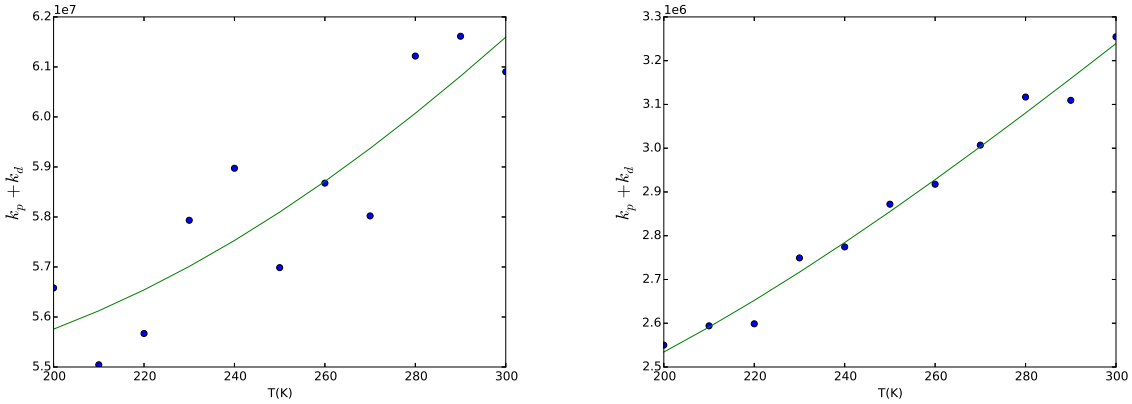

(a) 4CzIPN, $r_1 + r_2$

(b) m-MTDATA:t-Bu-PBD, $r_1 + r_2$

FIG. 6: Fit for combined delayed and prompt relaxation constants ($r_1 + r_2$). Data are from supplemental materials provided by Goushi, et. al.[3] and Uoyama, et. al.[4]. The 4CzIPN fit exhibits scatter in the prompt relaxation time measurements compared to the reduced scatter in the m-MTDATA:t-Bu-PBD prompt relaxation time data.

and the ΔE_{S-T} value agrees more closely with ours. Thus, in these two examples differences in ΔE_{S-T} seem to follow the k_{risc} calculation in the earlier method, rather than the scatter in decay rates.

IV. CONCLUSIONS

In this work we have obtained closed solutions for steady state and transient behaviors in TADF systems and described a procedure for extracting the primary relaxation and crossing rates, and the prefactor and gap energy from temperature dependent prompt and delayed decay rates. We applied our method to data reported for two TADF materials and used the fitted values for the primary rate constants to calculate their fluorescence/phosphorescence and singlet/triplet population ratios. The primary rate constants obtained in this manner are in reasonable agreement with reported values where available, and we are able to report the fluorescence/phosphorescence ratios 37:1 for 4CzIPN and 47:1 for m-MTDATA:t-Bu-PBD, along with their singlet/triplet population ratios 0.13 and 0.53. It is hoped that the method will be useful in studies of TADF and OLEDS.

[1] A. Endo, K. Sato, K. Yoshimura, T. Kai, A. Kawada, H. Miyazaki and C. Adachi, Appl. Phys. Lett. 98, 093302 (2011)

[2] J. R. Kirchhoff, R. E. Gamache, Jr., M. W. Blaskie, A. A. Del Paggio, R. K. Lengel and D. R. McMillin, Inorg. Chem 22, 2380-2384 (1983)

[3] K. Goushi, K. Yoshida, K. Sato and C. Adachi, Nature Photonics 6, 253 (2012)

[4] H. Uoyama, K. Goushi, K. Shizu, H. Nomura and C. Adachi, Nature 492, 234 (2012)

[5] F. B. Dias, K. N. Bourdakos, V. Jankus, K. C. Moss, K. T. Kamtekar, V. Bhalla, J. Santos, M. R. Bryce and A. P. Monkman, Adv. Mater. 25, 3707-3714 (2013)

[6] A. Niwa, T. Kobayashi, T. Nagase, K. Goushi, C. Adachi and H. Naito, Appl. Phys. Lett. 104, 213303 (2014)

[7] T. Chen, L. Zheng, J. Yuan, Z. An, R. Chen, Y. Tao, H. Li, X. Xie and W. Huang, Sci. Rep. 5, 10923 (2015)

[8] L. Bergmann, G. Hedley, T. Baumann, S. Bräse and I. D. W. Samuel, Sci. Adv. 2, e1500889 (2016)

[9] D. J. Gaspar, E. Polikarpov (eds.) *OLED Fundamentals: Materials, Devices, and Processing of Organic Light-Emitting Diodes*, (CRC Press, Boca Raton, 2014)

[10] *F*undamentals of Photochemistry, Revised Edition, K K Rohatgi-Mukherjee, New Age, New Delhi, 1978, page 133

[11] V. Lawetz, G. Orlandi and W. Siebrand, J. Chem. Phys. 56(8), 4058 (1972)

[12] Q. Peng, X. Li and F. Li, J. Appl. Phys. 112, 114512 (2012)

[13] M. C. Nelson, `arXiv:1601.04981 [physics.optics]` (2016)

[14] A. Pitarch, G. Garcia-Belmonte and J. Bisquert, J. Appl. Phys. 100, 084502 (2006)